J Appl Electrochem (2009) 39:429–438
DOI 10.1007/s10800-008-9688-y

ORIGINAL PAPER

# Evaluation of electrochemical frequency modulation as a new technique for monitoring corrosion and corrosion inhibition of carbon steel in perchloric acid using hydrazine carbodithioic acid derivatives

**K. F. Khaled**

Received: 19 March 2008 / Accepted: 7 October 2008 / Published online: 25 October 2008


**Abstract** Electrochemical frequency modulation, EFM is a new technique for corrosion rate measurements. With the EFM technique, the corrosion rate and corrosion kinetic parameters can be obtained instantaneously without prior knowledge of Tafel slopes, which makes this method an ideal technique for application as a corrosion monitoring tool. Results obtained with the EFM technique were shown to be in agreement with chemical (weight loss) and electrochemical methods (Tafel extrapolation and electrochemical impedance spectroscopy, EIS) for corrosion rate measurements. New synthesized hydrazine carbodithioic acid derivatives namely, *N*′-furan-2-yl-methylene-hydrazine carbodithioic acid (A), *N*′-(4-dimethylamino-benzylidene)-hydrazine carbodithioic acid (B) and *N*′-(3-nitro-benzylidene)-hydrazine carbodithioic acid (C) were examined as corrosion inhibitors for carbon steel in 1 M perchloric acid solution. The results obtained from both chemical and electrochemical measurements show that these compounds suppressed both anodic and cathodic processes of carbon steel corrosion in 1 M $HClO_4$ by adsorption on the electrode surface. The adsorption mode follows the Langmuir adsorption isotherm. The efficiency of the inhibitors increases in the order C > B > A.

**Keywords** Carbon steel · EFM · Impedance · Acid corrosion inhibition

K. F. Khaled (✉)
Electrochemistry Research Laboratory, Chemistry Department, Faculty of Education, Ain Shams University, Roxy, Cairo, Egypt
e-mail: khaledrice2003@yahoo.com

## 1 Introduction

Electrochemical frequency modulation, EFM is a nondestructive corrosion measurement technique that can directly give values of the corrosion current without prior knowledge of Tafel constants. Like EIS, it is a small signal ac technique. Unlike EIS, however, two sine waves (at different frequencies) are applied to the cell simultaneously. Because current is a non-linear function of potential, the system responds in a non-linear way to the potential excitation. The current response contains not only the input frequencies, but also, frequency components which are the sum, difference, and multiples of the two input frequencies.

This work is a continuation of previous work [1] on the evaluation of electrochemical frequency modulation, EFM, as a new non-linear distortion technique as well as development of new corrosion inhibitors for acidic solutions [2–6]. Recently, Bogaerts et al. proposed EFM as a novel technique for online corrosion monitoring [7, 8]. In this technique current responses due to a potential perturbation by one or more sine waves are measured at more frequencies than the frequency of the applied signal, for example at zero, harmonic and intermodulation frequencies. This simple principle offers various possibilities for corrosion rate measurements. With this novel EFM technique, the corrosion rate can be determined from the corrosion system responses at the intermodulation frequencies. The EFM approach requires only a small polarizing signal, and measurements can be completed in a short period of time. Another advantage of EFM is using the causality factors as a good internal check for verifying the validity of the data obtained by this technique. EFM used successfully for corrosion rate measurements for mild steel in acidic and neutral environment without and with inhibitors [8].

Kus and Mansfeld [9] evaluated the EFM technique for several corrosion systems including active and passive systems and found that EFM measurements can be applied successfully only for a limited number of corrosion systems with fairly high corrosion rates and the technique should be used only with great caution for corrosion monitoring.

In corrosion research, it is known that the corrosion process is non linear in nature, a potential distortion by one or more sine waves will generate responses at more frequencies than the frequencies of the applied signal. Virtually no attention has been given to the intermodulation or electrochemical frequency modulation; however, EFM has shown that this non-linear response contains enough information about the corroding system so that the corrosion current can be calculated directly. The theoretical background of the technique is presented elsewhere [7, 8].

The research presented in this paper will go one step further with the EFM technique, the EFM technique will be used here for online monitoring of the corrosion rate of carbon steel in 1 M perchloric acid in the absence and presence of new synthesized hydrazine carbodithioic acid derivatives namely, *N*′-furan-2-yl-methylene-hydrazine carbodithioic acid (A), *N*′-(4-dimethylamino-benzylidene)-hydrazine carbodithioic acid (B) and *N*′-(3-nitro-benzylidene)-hydrazine carbodithioic acid (C) as possible corrosion inhibitors. The technique will be evaluated by comparing corrosion inhibition data obtained by EFM with that obtained from traditional techniques like weight loss, Tafel extrapolation and EIS.

## 2 Experimental

### 2.1 Inhibitors

Inhibitors were synthesized in the laboratory following a procedure described elsewhere [6]. Hydrazine carbodithioic acid derivatives have been synthesized from equimolar of dithioic acid hydrazide and the corresponding aldehyde in absolute ethanol. The mixture was refluxed for 2 h then left to cool. The precipitate was filtered off and crystallized from ethanol to give the studied compounds. Figure 1 shows the method of preparation and the chemical structure for the studied compounds.

### 2.2 Electrodes

Coupons of commercial carbon steel (CS, composition in wt%: Cr = 0.012, Ni = 0.008, C = 0.08, Si = 0.02, P = 0.01, Fe = balance) with exposed surface area of 4 $cm^2$ (1, 1, 0.5 cm) were used for weight loss measurements. A carbon steel rod with the same composition was mounted in Teflon, and abraded using emery papers of 180, 120, 2/0, 4/0 grit size in order. It was polished with $Al_2O_3$ (0.5 μm particle size), cleaned in 18 MΩ cm water in an ultrasonic bath and rinsed with acetone and bi-distilled water. The same procedures were used with CS coupons in weight loss measurements. Electrochemical experiments were carried out under static conditions at 25 ± 1 °C in aerated molar perchloric acid solutions, in an electrolytic cell with a fine Luggin capillary tip placed close to the working electrode (WE) to minimize ohmic resistance.

### 2.3 Measurements

For weight loss measurements, the steel coupons were left hanging in the test solution for 2 h at 25 ± 1 °C before recording the loss in their weights. The corrosion rate was calculated in mg $cm^{-2}$ $h^{-1}$ on the basis of the apparent surface area. The inhibition efficiencies calculations were based on the weight loss measurements at the end of the exposure period. The results of the weight loss experiments were the mean of three runs, each with a fresh steel sheet and fresh acid solution. All the chemicals used for

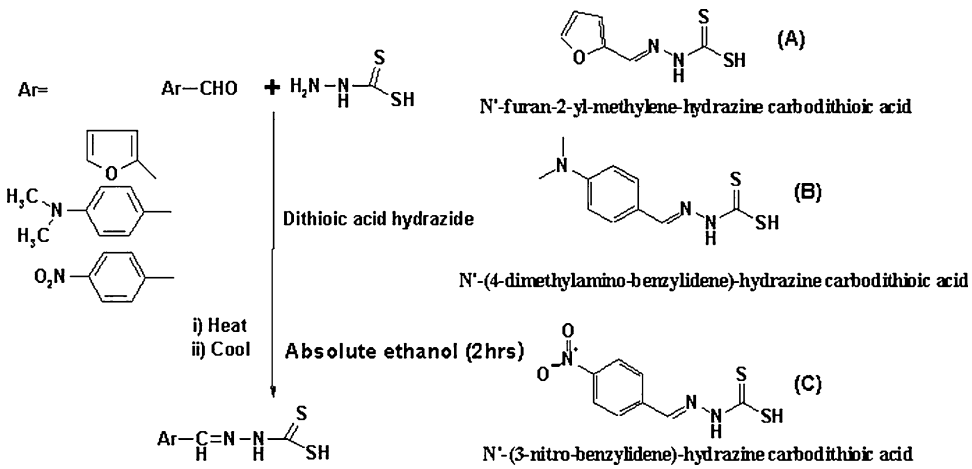


**Fig. 1** Preparation and chemical structure for hydrazine carbodithioic acid derivatives

preparation of the test solutions were of analytical grade. All electrochemical measurements were performed in a typical three-compartment glass cell consisted of carbon steel rod with a surface area of 0.28 $cm^2$, as working electrode (WE), platinum mesh as counter electrode (CE), and a saturated calomel electrode (SCE) as the reference electrode. Solutions were prepared from bi-distilled water. The electrode potential was allowed to stabilize for 60 min before starting the measurements. All experiments were conducted at 25 ± 1 °C using a water thermostat.

The electrodes were arranged in such a way that a one dimensional potential field existed over the WE surface in solution. To obtain information on the processes occurring at the CS/solution interface, Tafel curves were obtained by changing the electrode potential automatically from ($-250$ $mV_{SCE}$ to $+250$ $mV_{SCE}$) with a scan rate of 0.5 mV $s^{-1}$. EIS measurements were also carried out in the frequency range 100 kHz to 50 mHz with amplitude of 5 mV peak-to-peak using ac signals at the corrosion potential.

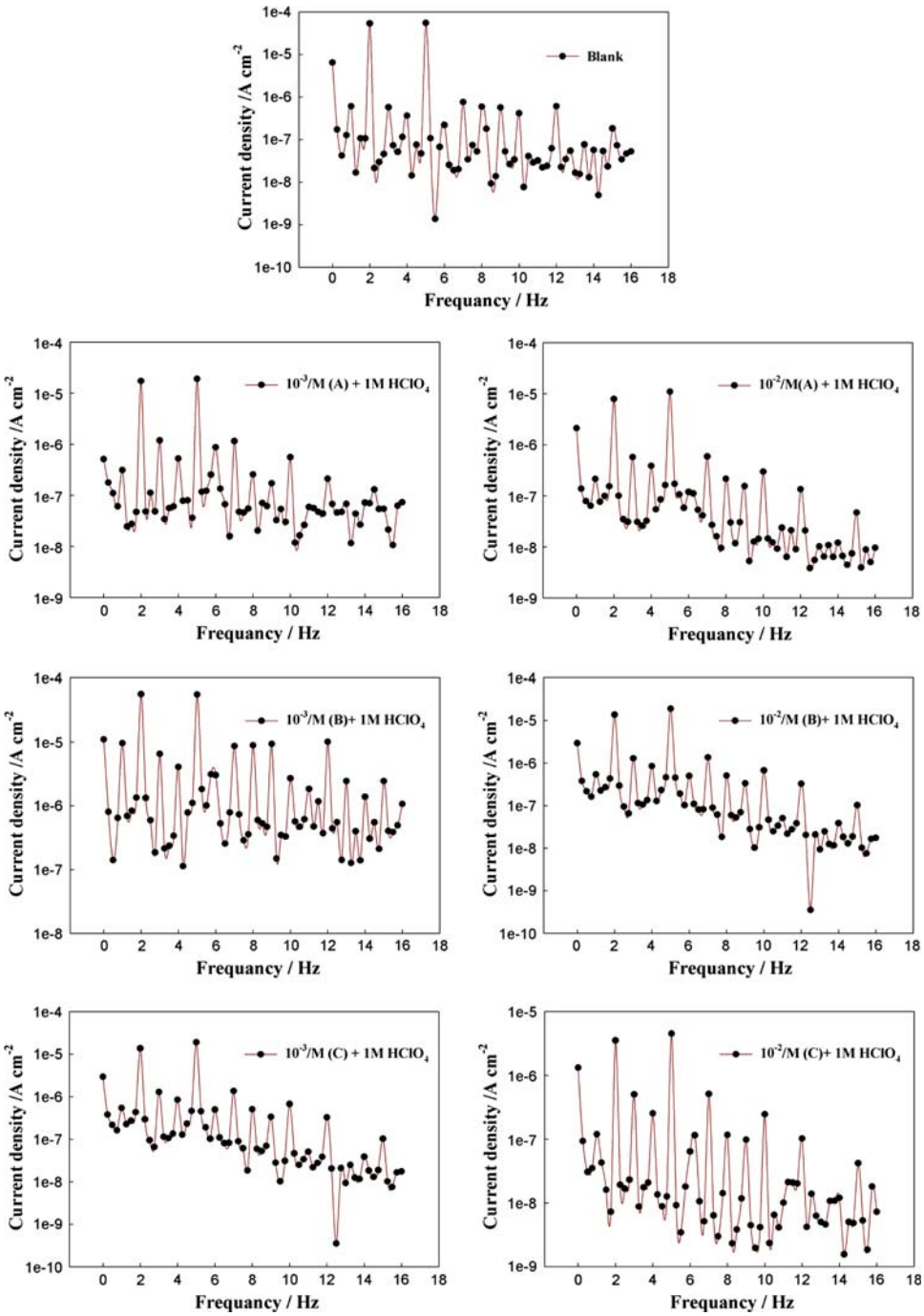


**Fig. 2** Intermodulation spectrum for carbon steel in 1 M $HClO_4$ in absence and presence of various concentrations of hydrazine carbodithioic acid derivatives at 25 ± 1 °C

Electrochemical frequency modulation, EFM, was carried out using two frequencies 2 and 5 Hz. The base frequency was 1 Hz, so the waveform repeated after 1 second. The higher frequency must be at least twice the lower one. The higher frequency must also, be sufficiently slow that the charging of the double layer does not contribute to the current response. Often, 10 Hz is a reasonable limit. Measurements were performed with a Gamry Instrument Potentiostat/Galvanostat/ZRA. This includes a Gamry framework system based on the ESA400, Gamry applications that include DC105 for dc corrosion measurements, EIS300 for electrochemical impedance spectroscopy measurements and EFM140 to calculate the corrosion current and Tafel constants. Along with a computer for collecting the data, Echem Analyst 4.0 software was used for plotting, graphing and fitting data.

## 3 Results and discussions

### 3.1 Electrochemical frequency modulation, EFM

Representative examples of the EFM experiments are presented in Fig. 2. Each plot is a spectrum, (an intermodulation spectrum).The two large peaks, with amplitudes of about 60 μA, are the response to the 2 and 5 Hz excitation frequencies. The peaks between 1 and 20 μA are the harmonics, sums, and differences of the two excitation frequencies. These peaks are used by the EFM140© software package to calculate the corrosion current and Tafel constants. It is important to note that, between the peaks the current response is very small. There is nearly no response (<100 nA) at 4.5 Hz, for example; the frequencies and amplitudes of the peaks are not coincident. They are direct consequences of EFM theory. Corrosion kinetic parameters were calculated from EFM techniques using Eqs. 1–5:

$$i_{\text{corr}} = \frac{i_{\omega}^2}{\sqrt{48(2i_{\omega}i_{3\omega} - i_{2\omega})}} \tag{1}$$

$$\beta_{\text{a}} = \frac{i_{\omega}U_o}{2i_{2\omega} + 2\sqrt{3}\sqrt{2i_{3\omega}i_{\omega} - i_{2\omega}^2}} \tag{2}$$

$$\beta_{\text{c}} = \frac{i_{\omega}U_o}{2\sqrt{3}\sqrt{2i_{3\omega}i_{\omega} - i_{2\omega}^2 - 2i_{2\omega}}} \tag{3}$$

$$\text{Causality factor (2)} = \frac{i_{\omega_2 \pm \omega_1}}{i_{2\omega_1}} = 2.0 \tag{4}$$

$$\text{Causality factor (3)} = \frac{i_{2\omega_2 \pm \omega_1}}{i_{3\omega_1}} = 3.0 \tag{5}$$

where $i$ is the instantaneous current density at the WE measured at frequency $\omega$ and $U_o$ amplitude of the sine wave distortion.

Table 1 shows the corrosion kinetic parameters, such as inhibition efficiency ($E_{\text{EFM}}$%), corrosion current density $i_{\text{corr}}$ (μA cm$^{-2}$), Tafel constants ($\beta_{\text{a}}$, $\beta_{\text{c}}$) and causality factors (CF-2, CF-3) at different concentrations of hydrazine carbodithioic acid derivatives in 1 M $HClO_4$ at 25 ± 1 °C. From Table 1 the corrosion current densities decrease with increasing concentration of these compounds. The inhibition efficiencies $E_{\text{EFM}}$% increase with increase in A, B and C concentration. The causality factors

**Table 1** Electrochemical kinetic parameters obtained by EFM technique for CS in absence and presence of various concentrations of hydrazine carbodithioic acid derivatives in 1 M $HClO_4$ at 25 ± 1 °C

| Inhibitor | Concentration/M | $i_{\text{corr}}$/μA cm$^{-2}$ | $\beta_{\text{a}}$/mV dec$^{-1}$ | $\beta_{\text{c}}$/mV dec$^{-1}$ | $E_{\text{EFM}}$/% | CF-2 | CF-3 |
|---|---|---|---|---|---|---|---|
| | Blank | 92.00 | 81.0 | 178.1 | – | 1.10 | 2.95 |
| Compound A | $10^{-4}$ | 46.10 | 69.5 | 181.5 | 49.8 | 1.45 | 2.68 |
| | $5 \times 10^{-4}$ | 38.80 | 79.4 | 181.5 | 57.8 | 2.01 | 2.25 |
| | $10^{-3}$ | 29.45 | 88.5 | 169.3 | 67.9 | 2.01 | 2.51 |
| | $5 \times 10^{-3}$ | 23.03 | 74.4 | 182.8 | 74.9 | 2.02 | 3.04 |
| | $10^{-2}$ | 13.85 | 74.4 | 175.8 | 84.9 | 1.70 | 2.15 |
| Compound B | $10^{-4}$ | 38.64 | 95.0 | 168.2 | 58.0 | 2.01 | 3.02 |
| | $5 \times 10^{-4}$ | 32.23 | 86.0 | 174.5 | 64.9 | 1.98 | 2.85 |
| | $10^{-3}$ | 23.10 | 79.5 | 168.4 | 74.8 | 2.02 | 3.04 |
| | $5 \times 10^{-3}$ | 14.73 | 90.3 | 174.5 | 83.9 | 1.85 | 1.33 |
| | $10^{-2}$ | 10.13 | 63.1 | 153.9 | 88.9 | 1.74 | 1.43 |
| Compound C | $10^{-4}$ | 34.97 | 79.4 | 165.5 | 61.9 | 2.00 | 2.25 |
| | $5 \times 10^{-4}$ | 27.61 | 86.5 | 184.6 | 69.9 | 1.93 | 2.74 |
| | $10^{-3}$ | 19.33 | 63.1 | 169.9 | 78.9 | 1.75 | 1.43 |
| | $5 \times 10^{-3}$ | 11.97 | 85.2 | 174.2 | 86.9 | 1.93 | 1.33 |
| | $10^{-2}$ | 4.61 | 60.5 | 159.3 | 94.9 | 2.02 | 2.03 |

in Table 1 are very close to the theoretical values which, according to EFM theory [7], should guarantee the validity of Tafel slopes and corrosion current densities. Corrosion inhibition efficiencies calculated from EFM data can be obtained from Eq. 6.

$$E_{\mathrm{EFM}}\% = \left(1 - \frac{i_{\mathrm{corr}}}{i^{0}_{\mathrm{corr}}}\right) \times 100 \qquad (6)$$

where $i^{0}_{\mathrm{corr}}$ and $i_{\mathrm{corr}}$ are corrosion current density in the absence and presence of the studied compounds, respectively.

The causality factors in Table 1 indicate that the measured data are of good quality. The standard values for CF-2 and CF-3 are 2.0 and 3.0, respectively. To evaluate the EFM technique as an effective corrosion monitoring technique, several traditional corrosion techniques were applied to study the corrosion inhibition of carbon steel by A, B and C compounds in 1 M $HClO_4$ solutions. EIS, Tafel extrapolation and weight loss measurements were used to calculate the inhibition efficiency as well as other corrosion kinetic parameters

### 3.2 Electrochemical impedance spectroscopy, EIS measurements

EIS measurements were carried out to evaluate the data obtained from EFM as well as the performance of this new class of compounds against the corrosion of carbon steel in 1 M $HClO_4$. Figures 3–5 show impedance spectra of uninhibited and inhibited CS in 1 M $HClO_4$. The impedance diagrams show a depressed semicircle. This behaviour has been described and discussed by many authors [10–12]. In all cases, it is found that the diameter of the capacitive loop increases with increase in A, B and C concentrations. The change in concentration of hydrazine carbodithioic

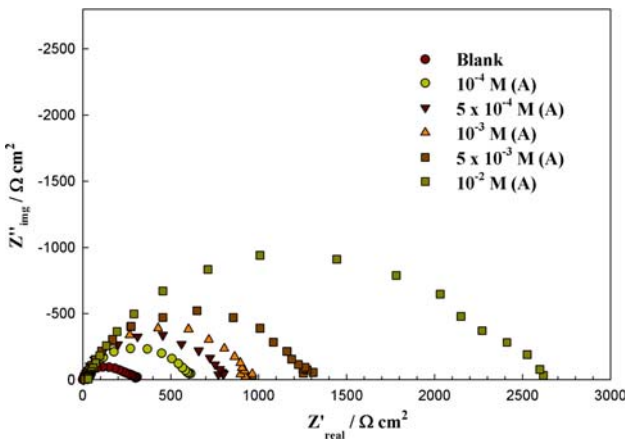


**Fig. 3** Complex plane impedance plots of CS in 1 M $HClO_4$ in absence and presence of various concentrations of compound (A) at 25 ± 1 °C

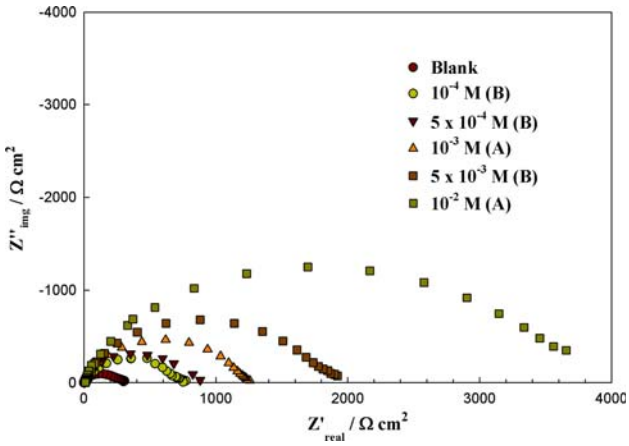


**Fig. 4** Complex plane impedance plots of CS in 1 M $HClO_4$ in absence and presence of various concentrations of compound (B) at 25 ± 1 °C

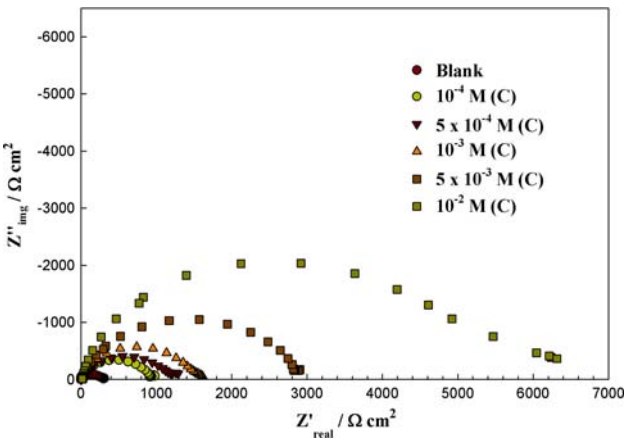


**Fig. 5** Complex plane impedance plots of CS in 1 M $HClO_4$ in absence and presence of various concentrations of compound (C) at 25 ± 1 °C

acid derivatives did not alter the shape of the impedance behaviour, suggesting that inhibition is accomplished by adsorption on the electrode surface without detectable changes in the chemistry of corrosion.

The measured complex plane impedance plots are similar to that calculated by the equivalent circuit models [3, 4]. The black spheres in Fig. 6 represent the experimental data while the solid lines represent the best fit obtained using the equivalent circuit in Fig. 7. A constant phase element CPE is used as a substitute for a capacitor in Fig. 7 to fit more accurately the impedance behaviour of the electrical double layer. Constant phase elements have widely been used to account for deviations brought about by surface roughness [3].

The impedance results were fitted using the Zview impedance analysis software (Scriber Associates Inc., Southern Pines, NC) [13]; the fitting parameters are listed in Table 2. The values of the charge-transfer resistance

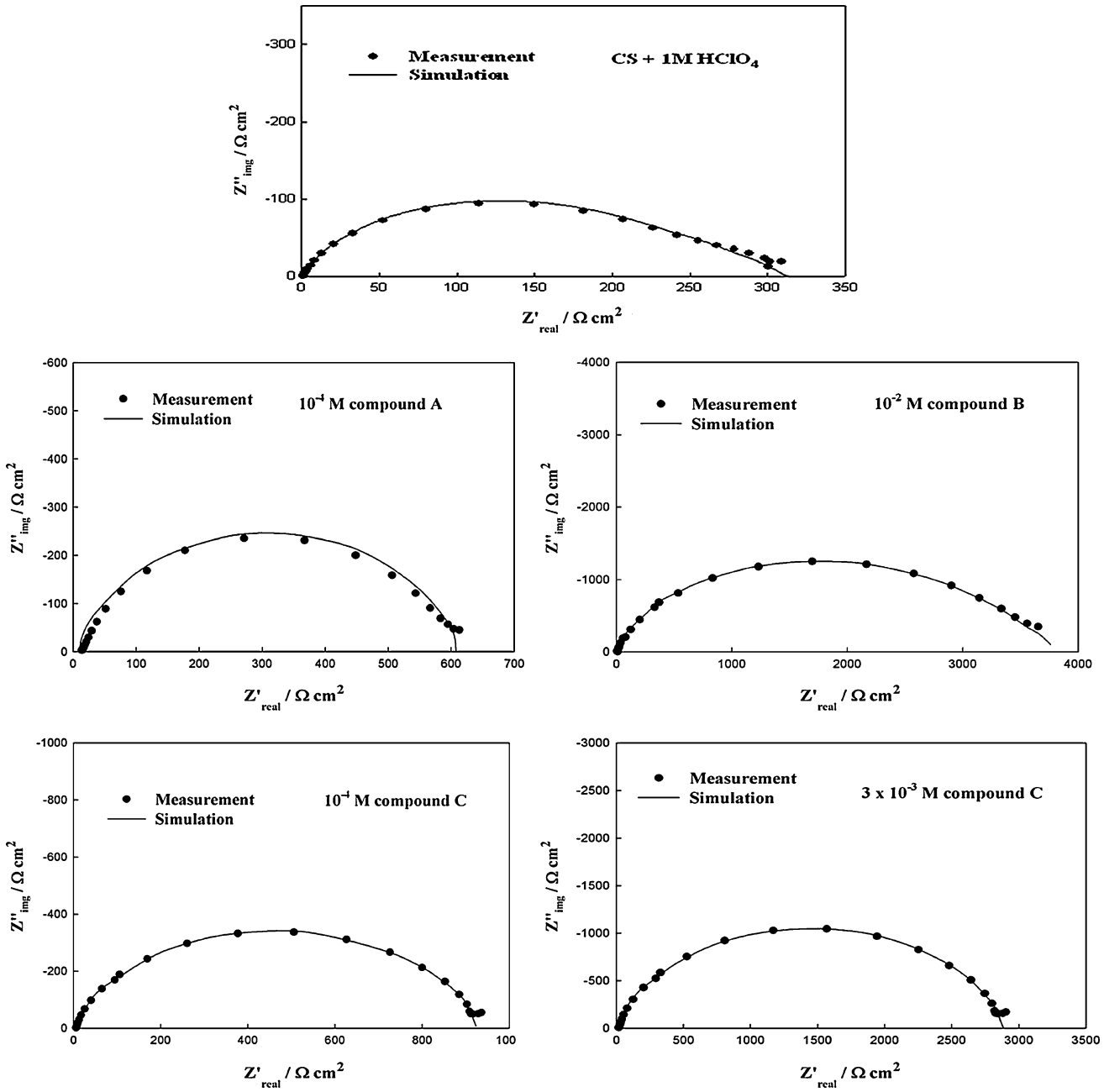


**Fig. 6** Measured and simulated complex plane impedance plots of CS corrosion in 1 M $HClO_4$ solutions at $E_{corr}$ in absence and presence of hydrazine carbodithioic acid derivatives at 25 ± 1 °C

increase, while those of CPE decrease with increase in inhibitor concentration. The decrease in CPE results from a decrease in local dielectric constant and/or an increase in the thickness of the double layer, suggesting that hydrazine carbodithioic acid derivatives inhibit the CS corrosion by adsorption at the CS/solution interface [14].

It is well known that the capacitance is inversely proportional to the thickness of the double layer [15]. A low capacitance may result if water molecules at the electrode interface are largely replaced by organic inhibitor molecules through adsorption [15]. The larger inhibitor molecules also reduce the capacitance through increase in the double layer thickness. The thickness of this protective layer increases with increasing inhibitor concentration. This process results in a noticeable decrease in CPE/$C_{dl}$ .This trend is in accordance with the Helmholtz model, given by Eq. 7.

$$C_{dl} = \varepsilon \varepsilon_o A/d \tag{7}$$

where d is the thickness of the protective layer, $\varepsilon$ is the dielectric constant of the medium, $\varepsilon_o$ is the vacuum permittivity and A is the effective surface area of the

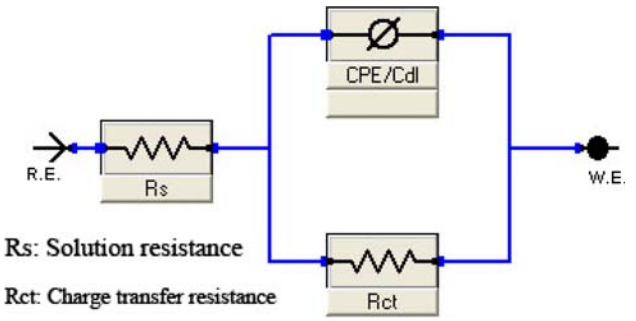


**Fig. 7** Equivalent circuit used to model impedance data in 1 M $HClO_4$ solutions

electrode. The value of CPE/$C_{dl}$ is always smaller in the presence of the inhibitor than in its absence, as a result of the effective adsorption of the inhibitor. It is apparent that a causal relationship exists between adsorption and inhibition [16].

The $R_{ct}$ values were used to calculate the $E_{imp}\%$ values (see Table 2) recorded for CS in 1 M $HClO_4$ solutions containing various concentrations of the tested inhibitors at 25 ± 1 °C, using Eq. 8:

$$E_{imp}\% = (1 - \frac{R^o_{ct}}{R_{ct}}) \times 100 \quad (8)$$

where $R^0_{ct}$ and $R_{ct}$ are the charge-transfer resistances for uninhibited and inhibited solutions, respectively. It is apparent that the inhibition efficiency increases with increase in concentration. It can be seen that compound C gave the best efficiency. Also, Table 2 shows that the corrosion inhibition efficiencies obtained from EIS measurements are in good agreement with those obtained from EFM.

### 3.3 Tafel polarization measurements

The values of the corrosion current density ($j_{corr}$), listed in Table 3, recorded for carbon steel without and with various concentrations of the studied compounds were determined by extrapolation of the cathodic and anodic Tafel lines to the corrosion potential ($E_{corr}$). Other electrochemical parameters, namely anodic and cathodic Tafel slopes ($\beta_a$, $\beta_c$) are also presented in Table 3. The inhibition efficiencies were evaluated from dc measurements using Eq. 9:

$$E_{Tafel}\% = (1 - \frac{j_{corr}}{j^o_{corr}}) \times 100 \quad (9)$$

where $j^0_{corr}$ and $j_{corr}$ are the corrosion current densities for uninhibited and inhibited solutions, respectively. As seen from Figs. 8–10, the anodic and cathodic reactions are affected by the hydrazine carbodithioic acid derivatives. Thus, hydrazine carbodithioic acid derivatives are mixed-type inhibitors. The addition of hydrazine carbodithioic acid derivatives to $HClO_4$ solutions reduces the anodic dissolution of CS and also retards the cathodic hydrogen evolution reaction. There is no definite shift of corrosion potential ($E_{corr}$), and $j_{corr}$ decreased when the concentration of hydrazine carbodithioic acid derivatives was increased. The inhibiting effect of the compounds may be related to their adsorption and the formation of a barrier film on the electrode surface.

It is obvious from Table 3 that the slopes of the anodic ($\beta_a$) and cathodic ($\beta_c$) Tafel lines remain almost unchanged upon addition of the compounds. Thus the adsorbed inhibitor acts by simple blocking of active sites for both anodic and cathodic processes. In other words, the inhibitor decreases the surface area for corrosion without affecting

**Table 2** Circuit element $R_s$, $R_{ct}$, $n$ and CPE values obtained using equivalent circuit in Fig. 7 for CS in 1 M $HClO_4$ in absence and presence of various concentrations of hydrazine carbodithioic acid derivatives

| Inhibitor | Concentration/M | $R_s$/Ω cm$^2$ | $R_{ct}$/Ω cm$^2$ | $n$ | CPE/μF cm$^{-2}$ | $E_{imp}$/% |
|---|---|---|---|---|---|---|
| | Blank | 2.2 | 313.4 | 0.93 | 39.3 | |
| Compound A | $10^{-4}$ | 2.3 | 628.8 | 0.91 | 24.8 | 50.16 |
| | $5 \times 10^{-4}$ | 3.1 | 827.0 | 0.85 | 18.9 | 62.11 |
| | $10^{-3}$ | 2.2 | 983.6 | 0.83 | 15.9 | 68.14 |
| | $5 \times 10^{-3}$ | 3.4 | 1311.2 | 0.87 | 11.9 | 76.09 |
| | $10^{-2}$ | 2.5 | 2626.3 | 0.79 | 5.9 | 88.06 |
| Compound B | $10^{-4}$ | 4.6 | 746.95 | 0.86 | 20.9 | 58.04 |
| | $5 \times 10^{-4}$ | 3.7 | 898.14 | 0.84 | 17.4 | 65.11 |
| | $10^{-3}$ | 5.5 | 1256.6 | 0.87 | 12.4 | 75.06 |
| | $5 \times 10^{-3}$ | 3.3 | 1968.2 | 0.85 | 7.9 | 84.07 |
| | $10^{-2}$ | 4.4 | 3938.5 | 0.79 | 3.9 | 92.04 |
| Compound C | $10^{-4}$ | 2.2 | 925.65 | 0.92 | 16.8 | 66.14 |
| | $5 \times 10^{-4}$ | 3.3 | 1258.6 | 0.94 | 12.4 | 75.09 |
| | $10^{-3}$ | 1.9 | 1659.0 | 0.98 | 9.4 | 81.11 |
| | $5 \times 10^{-3}$ | 3.7 | 2864.3 | 0.82 | 5.4 | 89.06 |
| | $10^{-2}$ | 4.5 | 6304.0 | 0.83 | 2.4 | 95.03 |

**Table 3** Electrochemical polarization parameters for CS in absence and presence of various concentrations of hydrazine carbodithioic acid derivatives in 1 M $HClO_4$ at 25 ± 1 °C

| Inhibitor | Concentration/M | $j_{corr}$/μA cm$^{-2}$ | $-E_{corr}$/mV | $\beta_a$/mV dec$^{-1}$ | $\beta_c$/mV dec$^{-1}$ | $E_{Tafel}$/% |
|---|---|---|---|---|---|---|
| | Blank | 79.00 | −424.5 | 45.98 | 171.6 | – |
| Compound A | $10^{-4}$ | 43.5 | −431.0 | 44.5 | 187.8 | 44.93 |
| | $5 \times 10^{-4}$ | 33.2 | −424.6 | 45.87 | 159.8 | 57.97 |
| | $10^{-3}$ | 27.6 | −420.7 | 49.52 | 175.3 | 65.06 |
| | $5 \times 10^{-3}$ | 21.3 | −419.8 | 47.9 | 195.5 | 73.04 |
| | $10^{-2}$ | 12.6 | −427.6 | 42.1 | 188.1 | 84.05 |
| Compound B | $10^{-4}$ | 35.5 | −419.7 | 55.66 | 179.6 | 55.06 |
| | $5 \times 10^{-4}$ | 30.0 | −423.6 | 53.2 | 187.9 | 62.03 |
| | $10^{-3}$ | 22.9 | −422.5 | 54.7 | 169.2 | 71.01 |
| | $5 \times 10^{-3}$ | 15.0 | −425.7 | 53.0 | 174.0 | 81.01 |
| | $10^{-2}$ | 8.7 | −410.3 | 58.2 | 185.4 | 88.98 |
| Compound C | $10^{-4}$ | 30.8 | −413.7 | 59.78 | 195.9 | 61.01 |
| | $5 \times 10^{-4}$ | 21.3 | −431.4 | 58.27 | 189.5 | 73.03 |
| | $10^{-3}$ | 17.4 | −428.0 | 54.8 | 189.8 | 77.97 |
| | $5 \times 10^{-3}$ | 11.1 | −421.5 | 55.8 | 187.3 | 85.95 |
| | $10^{-2}$ | 6.3 | −421.6 | 56.5 | 176.0 | 92.03 |

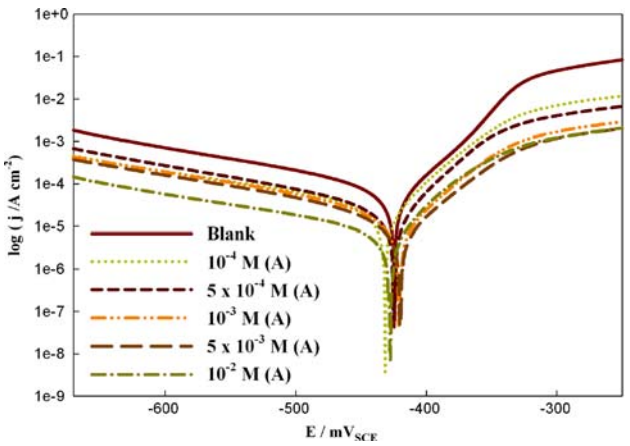


**Fig. 8** Anodic and cathodic Tafel polarization curves for CS in the absence and presence of various concentrations of compound (A) in 1 M $HClO_4$ at 25 ± 1 °C

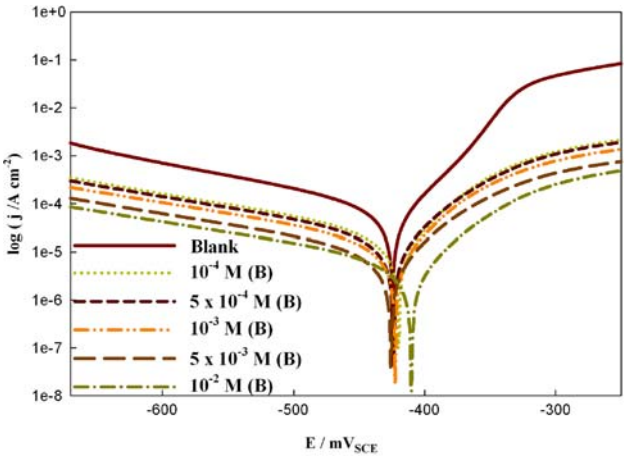


**Fig. 9** Anodic and cathodic Tafel polarization curves for CS in the absence and presence of various concentrations of compound (B) in 1 M $HClO_4$ at 25 ± 1 °C

the corrosion mechanism of carbon steel in perchloric acid solutions, and only causes inactivation of part of the surface with respect to the corrosive medium [16]. The kinetic parameters listed in Table 3 show good agreement with those obtained by EIS and EFM. Similar results were reported by Bosch et al. [7]. This is likely due to the fact that the entire bandwidth of EFM measurements was in the dc limit region of the impedance spectrum.

### 3.4 Weight loss measurements

Values of inhibition efficiency $E_w$% and corrosion rate (mg cm$^{-2}$ h$^{-1}$) obtained from the weight loss method at different concentrations of hydrazine carbodithioic acid derivatives at 25 ± 1 °C are summarized in Table 4. $E_w$% values, were calculated using Eq. 10:

$$E_w\% = \left(1 - \frac{w}{w^0}\right) \times 100 \quad (10)$$

where $w^0$ and $w$ are the weight loss in the absence and presence of hydrazine carbodithioic acid derivatives, respectively.

All the compounds inhibit the corrosion of carbon steel in 1 M $HClO_4$ solutions at all concentrations used. The inhibition efficiency increases with increase in concentration, Table 4. Figure 11 represents the inhibition

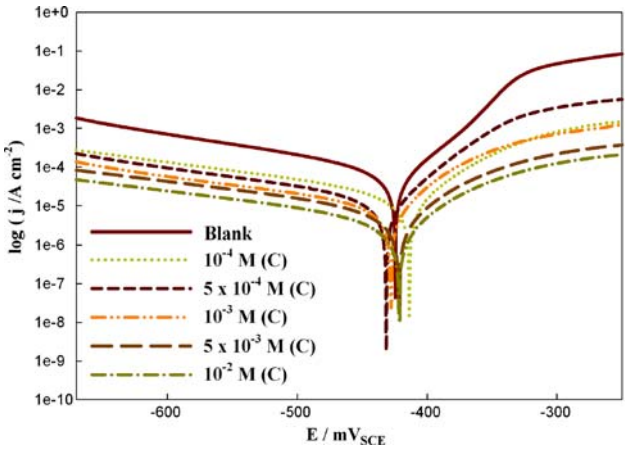


**Fig. 10** Anodic and cathodic Tafel polarization curves for CS in the absence and presence of various concentrations of compound (C) in 1 M $HClO_4$ at 25 ± 1 °C

**Table 4** Corrosion rate in mg cm$^{-2}$ h$^{-1}$, inhibition efficiency data and surface coverage $\theta$ obtained from weight loss measurements for CS in 1 M $HClO_4$ at 25 ± 1 °C in absence and presence of different concentrations of hydrazine carbodithioic acid derivatives

| Inhibitor | Concentration/ M | CR/ mg cm$^{-2}$ h$^{-1}$ | Surface coverage ($\theta$) | $E_w$/% |
|---|---|---|---|---|
| | Blank | 3.69 | – | – |
| Compound A | $10^{-4}$ | 1.62 | 0.56 | 56.1 |
| | $5 \times 10^{-4}$ | 1.33 | 0.64 | 63.9 |
| | $10^{-3}$ | 0.99 | 0.73 | 73.2 |
| | $5 \times 10^{-3}$ | 0.70 | 0.81 | 81.0 |
| | $10^{-2}$ | 0.33 | 0.91 | 91.0 |
| Compound B | $10^{-4}$ | 1.48 | 0.59 | 59.9 |
| | $5 \times 10^{-4}$ | 1.22 | 0.66 | 66.9 |
| | $10^{-3}$ | 0.81 | 0.78 | 78.0 |
| | $5 \times 10^{-3}$ | 0.40 | 0.89 | 89.2 |
| | $10^{-2}$ | 0.22 | 0.94 | 94.0 |
| Compound C | $10^{-4}$ | 1.14 | 0.69 | 69.1 |
| | $5 \times 10^{-4}$ | 0.70 | 0.81 | 81.0 |
| | $10^{-3}$ | 0.52 | 0.86 | 85.9 |
| | $5 \times 10^{-3}$ | 0.33 | 0.91 | 91.0 |
| | $10^{-2}$ | 0.11 | 0.97 | 97.0 |

efficiencies obtained for A, B and C at different concentrations using EFM, EIS, Tafel polarization and weight loss measurements. The calculated inhibition efficiency obtained from weight loss, Tafel polarization and EIS measurements are in good agreement with that obtained from EFM. The corrosion rates determined by EFM were higher, but still of the same order of magnitude as those obtained using other conventional electrochemical techniques. These results are in agreement with the literature [17].

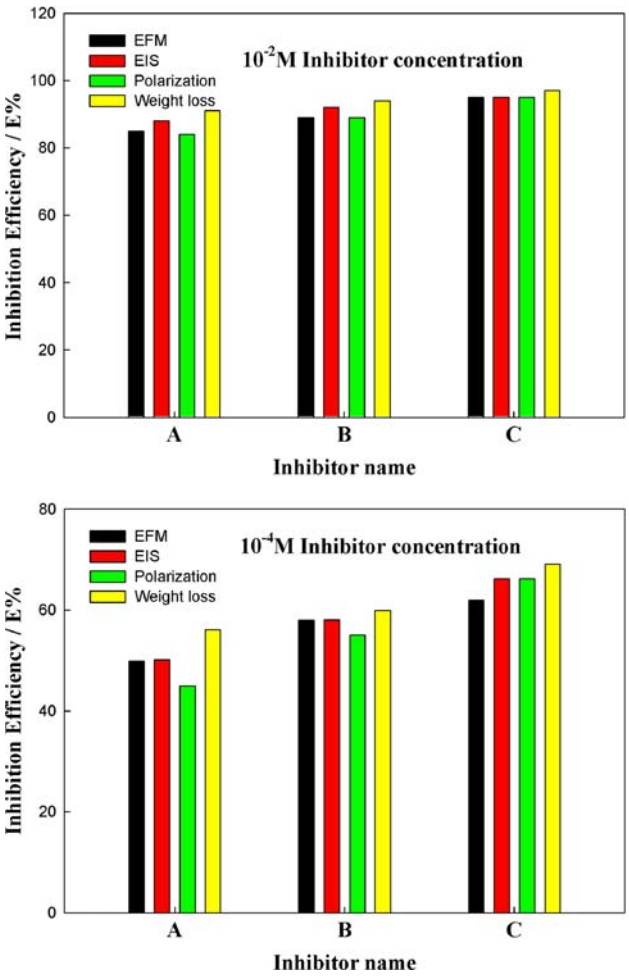


**Fig. 11** Comparison of inhibition efficiencies obtained with EFM, EIS, Tafel extrapolation and weight loss measurements at 25 ± 1 °C

### 3.5 Adsorption isotherm

The adsorption of an organic adsorbate on a metal surface is regarded as a substitutional adsorption process between the organic molecule in the aqueous solution ($Org_{(sol)}$), and water molecules adsorbed on the metallic surface ($H_2O_{(ads)}$) as follows [18]:

$$Org_{(sol)} + xH_2O_{(ads)} \leftrightarrow Org_{(ads)} + xH_2O_{(sol)} \quad (11)$$

where $x$ is the size ratio representing the number of water molecules replaced by one molecule of organic adsorbate.

The experimental data were tested with several adsorption isotherms. Surface coverage, $\theta$, was calculated in order to obtain the most appropriate isotherm. Surface coverage, $\theta$, was calculated from the weight loss measurements using Eq. 12:

$$\theta = 1 - \frac{w}{w^0} \quad (12)$$

where $w^0$ and $w$ are the weight loss in the absence and presence of inhibitor, respectively. The plots of log ($\theta$/

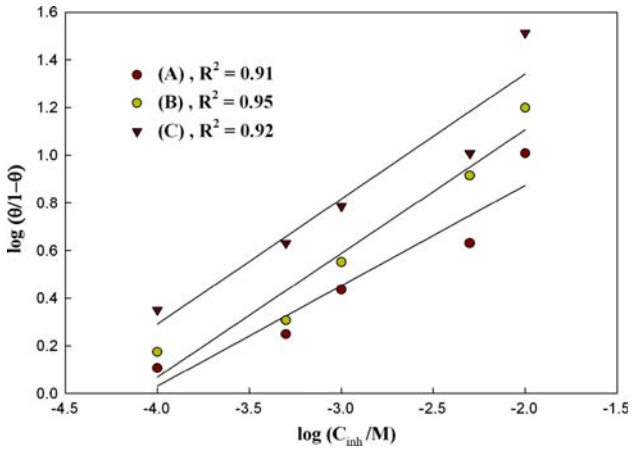


**Fig. 12** Langmuir adsorption plots for CS in various concentrations of hydrazine carbodithioic acid derivatives at 25 ± 1 °C

$(1 - \theta)$) versus log $C_{inh}$ yielded straight lines, where $C_{inh}$ is the inhibitor concentration. The best fit was obtained with Langumir adsorption isotherm as shown in Fig. 12. Adsorption of hydrazine carbodithioic acid derivatives on carbon steel can be achieved by two modes of adsorption: through the free lone pairs on nitrogen/sulphur and/or oxygen atoms, as well as the protonated species of these compounds as they are present in acidic medium and form cations which are electrostatically attracted to the pre-adsorbed chlorate anions on the steel surface.

## 4 Summary and conclusions

Since a corrosion process is a nonlinear electrochemical phenomenon, a potential perturbation signal by one or more sine waves will generate current responses at more frequencies than the frequencies of the applied signal. Electrochemical frequency modulation, EFM, measures the impedance of a corroding system over a narrow frequency range. Differing from the EIS technique, the amplitude of the signal in EFM can take different values at different frequencies. In order to obtain correct values of corrosion kinetic parameters using EFM, the entire frequency range of the EFM measurements has to fall within the dc limit of the impedance. Also, the system must show Tafel behaviour so that the mathematical relations between measured kinetic parameters and causality factors apply. Calculated corrosion rates from EFM data for the carbon steel/perchloric acid system were higher than those obtained from polarization measurements. Nevertheless, the causality factors were very close to their theoretical values. Also, the following conclusions can be drawn:

1. EFM can be used as a rapid and non destructive technique for corrosion rate measurements without prior knowledge of Tafel constants.
2. Inhibition efficiencies of the studied compounds increases with increasing inhibitor concentration and compound C shows the maximum inhibition compared with A and B.
3. Adsorption of the compounds obeys Langmuir adsorption isotherm.

**Acknowledgements** The author is grateful to Prof. Reda Mohammady Abdel-Rahman for preparation of the inhibitor molecules.

## References

1. Abdel-Rehim SS, Khaled KF, Abdel-Shafi NS (2006) Electrochim Acta 51:3267
2. Khaled KF (2006) Appl Surf Sci 252:4120
3. Khaled KF (2003) Electrochim Acta 48:2493
4. Khaled KF, Hackerman N (2003) Electrochim Acta 48:2715
5. Khaled KF, Hackerman N (2003) Electrochim Acta 49:485
6. Khaled KF (2004) Appl Surf Sci 230:307
7. Bosch RW, Hubrecht J, Bogaerts WF, Syrett BC (2001) Corrosion 57:60
8. Bosch RW, Bogaerts WF (1996) Corrosion 52:204
9. Kus E, Mansfeld F (2006) Corros Sci 48:965
10. Abdel-Rehim SS, Hassan HH, Amin MA (2002) Appl Surf Sci 187:279
11. Barcia OE, Mattos OR, Pebere N, Tribollet B (1993) J Electrochem Soc 140:2825
12. Deslouis C, Tribollet B, Mengoli G, Musiani MM (1988) J Appl Electrochem 18:374
13. Macdonald JR (1977) Impedance spectroscopy. Wiley, New York
14. Lagrenee M, Mernari B, Bouanis M, Traisnel M (2002) Corros Sci 44:573
15. Li P, Lin JY, Tan KL, Lee JY (1997) Electrochim Acta 42:605
16. Amin MA, Abd El-Rehim SS, El-Sherbini EEF, Bayoumi RS (2007) Electrochim Acta 52:3588
17. Han L, Song S (2008) Corros Sci 50:1551
18. Damaskin BB, Petrii OA, Batraktov B (1971) Adsorption of organic compounds on electrodes. Plenum, New York